PFC design method for SAC based on the stability theorem of the descriptor system and frequency response fitting

Masaya TANEMURA* and Yuichi CHIDA**

* Interdisciplinary Graduate School of Science and Technology, Shinshu University
4-17-1 Wakasato, Nagano-shi, Nagano 380-0928, Japan
E-mail: 15st208h@shinshu-u.ac.jp
** Faculty of Engineering, Shinshu University
4-17-1 Wakasato, Nagano-shi, Nagano 380-0928, Japan

Received 16 August 2013

Abstract
Simple adaptive control (SAC) is a control method that maintains control performance despite perturbations of a plant. However, there is a problem in that the vibratory output occurs in the transient response when SAC is applied to a vibration system which includes anti-resonance modes. The occurrence of the output depends on the structure of SAC and the output is caused by the vibratory input corresponding to the anti-resonance frequency. In order to overcome the problem, a method using an appropriate parallel feedforward compensator (PFC) is proposed. In the proposed method, an effective PFC is designed such that the gain of an augmented system is matched to that of a desired model under the ASPR condition of the augmented system. A design problem is described by LMI/BMI conditions. The problem using LMI/BMI conditions is solved by an iterative procedure. However, the leading coefficient of the PFC must be given a priori in order to guarantee the ASPR property, which provides some restrictions for applications of the proposed method. In the present paper, an improved method to overcome the abovementioned restrictions is proposed using the stability theorem of the descriptor system. The effectiveness of the proposed method is verified through numerical simulations and experiments.

Key words : Simple Adaptive Control, Parallel Feedforward Compensator, Frequency Response Fitting, Descriptor System, LMI, Vibration System

1. Introduction

Adaptive control is a control method that maintains control performance even if the plant properties change. In particular, simple adaptive control (SAC) includes high robustness and can be designed easily for applications. The effectiveness of SAC has been demonstrated experimentally in numerous plants (Hino, et al., 1992; Kyoizumi, et al., 2001, Ohtomo, et al., 1997). However, there is a problem in that the vibratory output occurs in transient responses when SAC is applied to a vibration system which includes anti-resonance modes (Yamashiro and Chida, 2012). The occurrence of the output depends on the structure of SAC, and the output is generated by the vibratory input corresponding to the anti-resonance frequency. In order to overcome the problem, a method using an appropriate parallel feedforward compensator (PFC) has been proposed (Yamashiro and Chida, 2012), in which a solution of the problem is to increase the gain of the PFC in the anti-resonance frequency band of the plant such that an augmented system consisting of the plant and PFC does not include the anti-resonance frequency. In such a case, the PFC must be designed so as to guarantee the gain property, as well as several conditions for SAC design, such as the almost strictly positive real (ASPR) conditions. One PFC design method for such a scenario for a continuous-time LTI SISO system was proposed by Tanemura, et al. (2013). In their method, the PFC is designed such that the gain of the augmented system is matched to that of a desired model. The matching condition is described using LMI/BMI conditions, and a desirable PFC is obtained by solving an optimization problem described by LMI/BMI conditions. The restrictions for the ASPR property are described as the LMI/BMI conditions and are included in the problem. In the restrictions, the minimum phase property of the augmented system is described by the Lyapunov inequality by Tanemura, et al. (2013). In such a case, the leading coefficient of the numerator of the PFC is assumed to be given a priori. However, it is difficult to obtain the leading coefficient in advance in some cases. The present paper introduces descriptor systems in order to overcome the restrictions. The description of a descriptor system possesses redundancy compared with the state space representation. Then, the stability theorem of a descriptor system proposed by Uezato and Ikeda (1998) is used in order to guarantee the minimum phase property of the augmented system. The proposed method requires no a priori information on the coefficients of the PFC, which are determined automatically in the proposed method because of redundancy of a descriptor system. On the other hand, a useful design method has been proposed by Mizumoto, et al. (2010). The method employs the desired model minus the plant as the PFC. The method can easily design the PFC without optimized calculation. However, if the order of the plant or the desired model is high, the order of the PFC increases because it depends on the order of the plant and the desired model. In contrast, the proposed method can design a low order PFC compared with the method proposed by Mizumoto, et al. (2010). The effectiveness of the proposed method is verified through not only simulations but also experiments using a mechanical vibration system. In addition, the robustness of the proposed design method is discussed in the present paper.

2. Problem statement

2.1. Plant

The present paper investigates the following continuous-time LTI SISO plant:

$$G_p(s)\begin{cases}\dot{\boldsymbol{x}}_p(t) = \boldsymbol{A}_p\boldsymbol{x}_p(t) + \boldsymbol{b}_p u_p(t)\\ y_p(t) = \boldsymbol{c}_p\boldsymbol{x}_p(t)\end{cases} \tag{1}$$
$$\boldsymbol{A}_p \in R^{n_p\times n_p},\ \boldsymbol{b}_p \in R^{n_p\times 1},\ \boldsymbol{c}_p \in R^{1\times n_p}$$

where $R^{n\times m}$ denotes an n-by-m real matrix set. The plant is assumed to be $(\boldsymbol{A}_p, \boldsymbol{b}_p)$-controllable and $(\boldsymbol{c}_p, \boldsymbol{A}_p)$-observable. The nominal parameters of $G_p(s)$ are assumed to be known.

2.2. Design of the SAC

An n_m-th order SISO reference model, which is a design parameter, is described as follows:

$$G_m(s)\begin{cases}\dot{\boldsymbol{x}}_m(t) = \boldsymbol{A}_m\boldsymbol{x}_m(t) + \boldsymbol{b}_m u_m(t)\\ y_m(t) = \boldsymbol{c}_m\boldsymbol{x}_m(t)\end{cases} \tag{2}$$
$$\boldsymbol{A}_m \in R^{n_m\times n_m},\ \boldsymbol{b}_m \in R^{n_m\times 1},\ \boldsymbol{c}_m \in R^{1\times n_m}$$

where $\boldsymbol{A}_m$ is a stable matrix. The control objective is for the output of the plant to follow that of the reference model. The following are the assumptions regarding the plant and the reference model used to design the SAC.

Assumptions (Mizumoto and Iwai, 2001)

1) The plant has ASPR characteristics.
2) The plant and the reference model have command generator tracker (CGT) solutions.
3) $u_m(t)$ is differentiable.

The ASPR property is defined as follows.

Definition (Mizumoto and Iwai, 2001)

$G_p(s)$ has ASPR property when a static output feedback that a closed-loop system with the static output feedback becomes strictly positive real exists.

Sufficient conditions of the ASPR property are described at the section of 3.2. A lot of plants hardly have the ASPR property of Assumption 1). A PFC is generally introduced in order to satisfy Assumption 1). The PFC is designed to ensure that the augmented system

$$G_a(s) := G_p(s) + G_f(s) \tag{3}$$

has ASPR characteristics. Where, $G_f(s)$ is the transfer function of the PFC. Since $G_a(s)$ is ASPR, SAC can be applied to $G_a(s)$. The control objective is to satisfy the following equation under the above assumptions:

$$\lim_{t\to\infty} e_a(t) = 0,\ \ e_a(t) = y_a(t) - y_m(t) \tag{4}$$

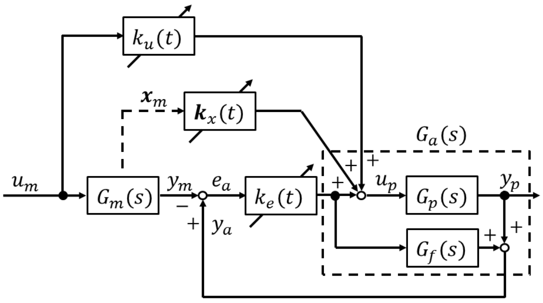

Fig. 1 This block diagram expresses the SAC system with the PFC. $G_p(s)$, $G_f(s)$, and $G_m(s)$ are the plant, PFC, and the reference model, respectively. $k_u(t)$ and $\boldsymbol{k}_x(t)$ are adaptive feedforward gains, and $k_e(t)$ is an adaptive feedback gain.

Where, $y_a(t)$ is the output of $G_a(s)$.

A block diagram of the SAC system is shown in Fig. 1. The SAC is described by the following equations:

$$u_p(t) = \boldsymbol{k}(t)^{\mathrm{T}}\boldsymbol{z}(t) \tag{5}$$

$$\boldsymbol{z}(t) = \begin{bmatrix} e_a(t) & \boldsymbol{x}_m(t)^{\mathrm{T}} & u_m(t) \end{bmatrix}^{\mathrm{T}}$$

$$\boldsymbol{k}(t) = \begin{bmatrix} k_e(t) & \boldsymbol{k}_x(t)^{\mathrm{T}} & k_u(t) \end{bmatrix}^{\mathrm{T}}$$

$$\boldsymbol{k}(t) = \boldsymbol{k}_P(t) + \boldsymbol{k}_I(t) \tag{6}$$

$$\boldsymbol{k}_P(t) = -\boldsymbol{\Gamma}_P\boldsymbol{z}(t)e_a(t) \tag{7}$$

$$\dot{\boldsymbol{k}}_I(t) = -\boldsymbol{\Gamma}_I\boldsymbol{z}(t)e_a(t) - \sigma(t)\boldsymbol{k}_I(t) \tag{8}$$

$$\sigma(t) = \frac{e_a^2(t)}{1+e_a^2(t)}\sigma_1 + \sigma_2 \tag{9}$$

$$\boldsymbol{\Gamma}_P = \boldsymbol{\Gamma}_P^{\mathrm{T}} > 0, \quad \boldsymbol{\Gamma}_I = \boldsymbol{\Gamma}_I^{\mathrm{T}} > 0, \quad \sigma_1 > 0, \quad \sigma_2 \geq 0$$

where $k_u(t)$ and $\boldsymbol{k}_x(t)$ are adaptive feedforward gains, and $k_e(t)$ is an adaptive feedback gain. The PI-type adaptive law using the σ-modification method is used as the adaptive adjusting law. Here, $\boldsymbol{\Gamma}_P$ and $\boldsymbol{\Gamma}_I$ are adaptive adjusting gain matrixes. $\boldsymbol{k}_I(t)$ stabilizes the SAC control system. $\boldsymbol{k}_P(t)$ plays a role in suppressing vibration of convergence of adaptive gains. The initial value of $\boldsymbol{k}_I(t)$ is a design parameter.

2.3. Vibratory input problem

The vibratory input problem is described in (Yamashiro and Chida, 2012) and (Tanemura, et al., 2015). An example of vibratory inputs is shown in Fig. 2 (Tanemura, et al., 2015). The two responses in Fig. 2 correspond to the two different PFCs, $G_{f1}(s)$ and $G_{f2}(s)$, which are indicated in Fig. 3. As shown in Fig. 3, the gain of $G_{f2}(s)$ is larger than that of $G_{f1}(s)$. The augmented system, $G_{a1}(s)$, for $G_{f1}(s)$ includes the anti-resonance, whereas the augmented system, $G_{a2}(s)$, for $G_{f2}(s)$, does not include the anti-resonance. The anti-resonance of $G_{a1}(s)$ causes the vibratory input in Fig. 2, and the input produces undesirable vibratory output. One method by which to avoid injecting the vibratory input is to specify the PFC for which the gain at the anti-resonance frequency is sufficiently high, e.g., $G_{f2}(s)$.

2.4. PFC design problem

The design problem considered in the present paper is such that the PFC includes sufficiently large gain in the specified frequency band and $G_a(s)$, which is an augmented system derived by the PFC, satisfies the ASPR conditions. Furthermore, the PFC is expected to be stable. The problem considered in the present paper is to design a PFC described by

$$G_f(s) := \frac{n_f(s)}{d_f(s)} := \frac{b_m s^m + b_{m-1}s^{m-1} + \cdots + b_0}{s^n + a_{n-1}s^{n-1} + \cdots + a_0}. \tag{10}$$

The design parameters are the degree of $G_f(s)$, n, m, and the coefficients a_i and b_i. Both n and m are assumed to be specified in advance, and a_i and b_i are assumed to be determined using the proposed method. The plant, $G_p(s)$, and the augmented system, $G_a(s) := G_p(s) + G_f(s)$, are assumed to be given as follows:

$$G_p(s) := \frac{n_p(s)}{d_p(s)} := \frac{b_{p_{m_p}} s^{m_p} + b_{p_{m_p-1}}s^{m_p-1} + \cdots + b_{p_0}}{s^{n_p} + a_{p_{n_p-1}}s^{n_p-1} + \cdots + a_{p_0}}, \tag{11}$$

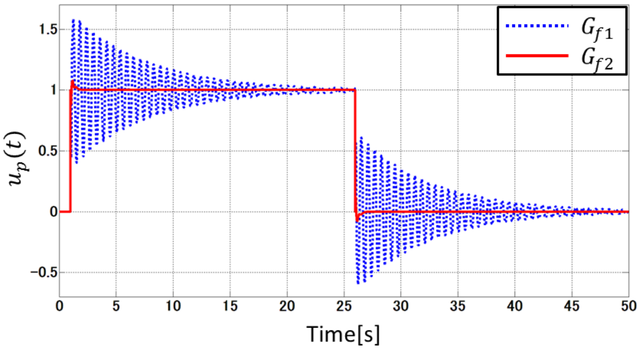

Fig. 2 Time history of $u_p(t)$ for $G_{f1}(s)$ and $G_{f2}(s)$ are expressed. Vibration of $u_p(t)$ for $G_{f2}(s)$ can be suppressed compared with $G_{f1}(s)$ because the augmented system, $G_{a2}(s)$, for $G_{f2}(s)$ does not include the anti-resonance.

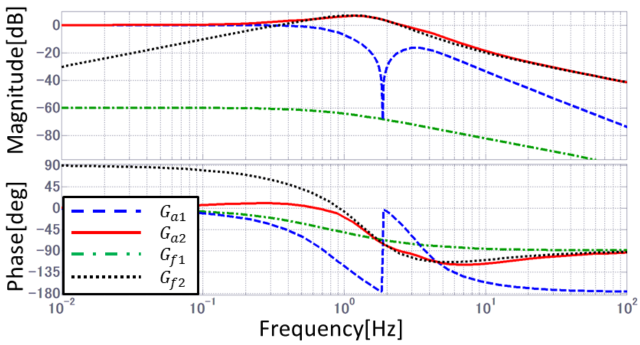

Fig. 3 Bode plots of $G_{a1}(s)$, $G_{a2}(s)$, $G_{f1}(s)$, and $G_{f2}(s)$ are expressed. The broken, solid, dotted, and chained lines are $G_{a1}(s)$, $G_{a2}(s)$, $G_{f1}(s)$, and $G_{f2}(s)$, respectively.

$$G_a(s) := \frac{n_a(s)}{d_a(s)} := \frac{d_f(s)n_p(s) + d_p(s)n_f(s)}{d_p(s)d_f(s)} = \frac{b_{a_{m_a}} s^{m_a} + b_{a_{m_a-1}} s^{m_a-1} + \cdots + b_{a_0}}{d_p(s)d_f(s)}. \tag{12}$$

3. Conventional method and associated problem

3.1. Outline

A design method of the PFC which avoids the vibratory input problem has been proposed by Tanemura, et al. (2013). The procedure of the method consists of the following two steps.

Step 1 A desired model, $G_r(s)$, is specified. $G_r(s)$ has sufficiently high gain in the anti-resonance frequency band of the plant, $G_p(s)$.

Step 2 The PFC, $G_f(s)$, is designed such that the frequency response of $G_a(s)$ matches $G_r(s)$ as closely as possible.

In Step 2, $G_f(s)$ is obtained by solving an optimization problem using LMI/BMI conditions. The ASPR condition of $G_a(s)$ and the stability condition of $G_f(s)$ are assessed using some constraints of the problem. The problem is solved using an iterative procedure. In one of the constraints for the ASPR conditions of $G_a(s)$, a priori information is required, such that the coefficient of the highest order of the numerator polynomial is known. However, this condition is strict in some cases and must be relaxed.

3.2. Conditions of the ASPR property of $G_a(s)$

The sufficient condition of the ASPR property of $G_a(s)$ is described as follows (Mizumoto and Iwai, 2001):

I) Relative degree of $G_a(s)$ is 0 or 1, $(n + n_p) - m_a = 0$ or 1.

II) $G_a(s)$ is a minimum phase system.

III) The leading coefficient of $G_a(s)$, $b_{a_{m_a}}$, is positive.

Condition I) is satisfied when the relative degree of the PFC is 1 and corresponds to Eq. (10) with $m = n - 1$. Condition II) is satisfied if and only if the polynomial of the numerator of $G_a(s)$,

$$n_a(s) = d_f(s)n_p(s) + d_p(s)n_f(s) = b_{a_{m_a}} s^{m_a} + \cdots + b_{a_i} s^i + \cdots + b_{a_0} \tag{13}$$

is stable. All $b_{a_0}, \cdots, b_{a_i}, \cdots, b_{a_{m_a}}$ in Eq. (13) consist of parameters, a_i and b_i, which are design parameters in Eq. (10) and are described as affine for a_i and b_i. The stability condition of $n_a(s)$ can be described using the controllability canonical form. If $b_{a_{m_a}} \neq 0$, the controllability canonical form of a transfer function for which the denominator is $n_a(s)$ is given by

$$\dot{\boldsymbol{x}}_a(t) = \boldsymbol{A}_a \boldsymbol{x}_a(t) + \boldsymbol{b}_a u_a(t), \tag{14}$$

$$\boldsymbol{A}_a = \begin{bmatrix} 0 & 1 & 0 & \cdots & 0 \\ 0 & 0 & 1 & \cdots & 0 \\ \vdots & \vdots & \ddots & \ddots & \vdots \\ 0 & 0 & \cdots & \cdots & 1 \\ -\frac{b_{a_0}}{b_{a_{m_a}}} & -\frac{b_{a_1}}{b_{a_{m_a}}} & \cdots & \cdots & -\frac{b_{a_{m_a-1}}}{b_{a_{m_a}}} \end{bmatrix}, \ \boldsymbol{b}_a = \begin{bmatrix} 0 \\ 0 \\ \vdots \\ 0 \\ \frac{1}{b_{a_{m_a}}} \end{bmatrix}. \tag{15}$$

The system of Eq. (14) is stable if and only if there exists a matrix $\boldsymbol{P}_a$ which satisfies

$$\boldsymbol{P}_a\boldsymbol{A}_a + \boldsymbol{A}_a^{\mathrm{T}}\boldsymbol{P}_a < 0,\ \boldsymbol{P}_a > 0. \tag{16}$$

By finding $\boldsymbol{P}_a$ and $\boldsymbol{A}_a$ in Eq. (16) at the same time, condition II) is guaranteed. In this case, Eq. (16) is not an LMI condition but rather a BMI condition for $\boldsymbol{A}_a$ and $\boldsymbol{P}_a$. If $\boldsymbol{A}_a$ is a known constant matrix, Eq. (16) can be solved as LMI for $\boldsymbol{P}_a$. On the other hand, if $\boldsymbol{P}_a$ is a known constant matrix, Eq. (16) can be solved as a LMI for $\boldsymbol{A}_a$. Thus, the above two procedures are executed iteratively to solve the BMI problem as LMIs. However, there is another difficulty in solving the problem such that Eq. (15) is not affine for a design parameter of $1/b_{a_{m_a}}$ in $\boldsymbol{A}_a$. In order to modify $\boldsymbol{A}_a$ to be affine, it is assumed that $b_{a_{m_a}}$ is given a priori and a specified fixed constant is used for $b_{a_{m_a}}$. Here, $b_{a_{m_a}}$ consists of b_{n-1}, as follows:

$$b_{a_{m_a}} = \begin{cases} b_{p_{m_p}} + b_{n-1} & (\gamma_p = 1) \\ b_{n-1} & (\gamma_p \geq 2)\ , \end{cases} \tag{17}$$

where $\gamma_p := n_p - m_p$ is the relative degree of $G_p(s)$. $b_{p_{m_p}}$ is a parameter of $G_p(s)$ and is given. However, b_{n-1} is a design parameter and so must be given a priori. Then, parameters b_{a_i}, with the exception of $b_{a_{m_a}}$, are affine for $a_0, \ldots, a_{n-1}, b_0, \ldots, b_{n-2}$. Note that, in the conventional method, $b_{a_{m_a}}$ must be specified in advance. However, since a suitable value of the leading coefficient, b_{n-1}, cannot be given in realistic situations, $b_{a_{m_a}}$ must be determined in an appropriate manner. Therefore, a modified method by which to overcome this requirement is proposed in the following section. Moreover, $b_{a_{m_a}}$ is specified to be positive in order to satisfy condition III).

3.3. Condition for frequency matching of $G_a(s)$ to $G_r(s)$

The desired model, described as $G_r(s)$, which does not include the anti-resonance, is specified for fitting the frequency responses of $G_a(s)$ and $G_r(s)$. By describing the matching condition using LMI, the PFC design problem becomes a convex optimization problem. In this case, $G_r(s)$ must be designed such that the anti-resonance is not included and the ASPR property is maintained. An error transfer function (Chida and Nishimura, 2008) is described as follows:

$$E(\omega) := M(\omega)G_r(j\omega) - M(\omega)\left(G_p(j\omega) + G_f(j\omega)\right) \tag{18}$$

where $M(\omega)$ is a frequency-dependent weighting function, and $G_p(s)$ and $G_f(s)$ are defined in Eq. (11) and (10). Equation (18) shows the matching error between $G_a(j\omega)$ and $G_r(j\omega)$, respectively. Equation (18) is, however, not affine with respect to parameters a_i, b_i. Thus, $M(\omega)$ is specified such that $M(\omega) = d_f(j\omega)/d(j\omega)$. Here, $d(j\omega)$ is a known polynomial of the n-th degree. Substituting $M(\omega) = d_f(j\omega)/d(j\omega)$ into Eq. (18) yields

$$\begin{aligned} E(\omega) &= \left(G_r(j\omega) - G_p(j\omega)\right)\frac{d_f(j\omega)}{d(j\omega)} - \frac{n_f(j\omega)}{d(j\omega)} \\ &= \frac{G_r(j\omega) - G_p(j\omega)}{d(j\omega)}\begin{bmatrix} 1 & j\omega & \cdots & (j\omega)^{n-1} & (j\omega)^n \end{bmatrix}\begin{bmatrix} a_0 \\ a_1 \\ \vdots \\ a_{n-1} \\ 1 \end{bmatrix} - \frac{1}{d(j\omega)}\begin{bmatrix} 1 & j\omega & \cdots & (j\omega)^{n-2} & (j\omega)^{n-1} \end{bmatrix}\begin{bmatrix} b_0 \\ b_1 \\ \vdots \\ b_{n-2} \\ b_{n-1} \end{bmatrix} \\ &= [\Phi_0^r(\omega) + \boldsymbol{\Phi}_a^r(\omega)\boldsymbol{a} + \boldsymbol{\Phi}_b^r(\omega)\boldsymbol{b}] + j[\Phi_0^i(\omega) + \boldsymbol{\Phi}_a^i(\omega)\boldsymbol{a} + \boldsymbol{\Phi}_b^i(\omega)\boldsymbol{b}] \\ &= E^r(\omega) + jE^i(\omega), \\ \boldsymbol{a} &:= [a_0, \ldots, a_{n-1}]^{\mathrm{T}},\ \ \boldsymbol{b} := [b_0, \ldots, b_{n-2}]^{\mathrm{T}} \end{aligned} \tag{19}$$

where Φ_0^r and Φ_0^i are independent terms of $\boldsymbol{a}$ and $\boldsymbol{b}$, $\boldsymbol{\Phi}_a^r$ and $\boldsymbol{\Phi}_a^i$ are terms of the coefficients of $\boldsymbol{a}$, and $\boldsymbol{\Phi}_b^r$ and $\boldsymbol{\Phi}_b^i$ are terms of the coefficients of $\boldsymbol{b}$. Assuming that $\boldsymbol{x}^{\mathrm{T}} := [\boldsymbol{a}^{\mathrm{T}}, \boldsymbol{b}^{\mathrm{T}}]$, which is a design vector, the affine equation for $\boldsymbol{x}$ is derived as follows:

$$\begin{aligned} \begin{bmatrix} E^r(\omega) \\ E^i(\omega) \end{bmatrix} &= \begin{bmatrix} \Phi_0^r(\omega) \\ \Phi_0^i(\omega) \end{bmatrix} + \begin{bmatrix} \boldsymbol{\Phi}_a^r(\omega) & \boldsymbol{\Phi}_b^r(\omega) \\ \boldsymbol{\Phi}_a^i(\omega) & \boldsymbol{\Phi}_b^i(\omega) \end{bmatrix}\boldsymbol{x} \\ &= \boldsymbol{\beta}(\omega) + \boldsymbol{\alpha}(\omega)\boldsymbol{x}. \end{aligned} \tag{20}$$

Equation (20) is intractable because Eq. (20) is a continuous function for ω. Therefore, errors in the discrete frequency data ω_k, which are sampled at N-points, are considered. Taking the discrete frequency data ω_k simplifies the problem.

The following error objective function J:

$$J(\boldsymbol{x}) := \sum_{k=1}^{N} \begin{bmatrix} E^r(\omega_k) & E^i(\omega_k) \end{bmatrix} \begin{bmatrix} E^r(\omega_k) \\ E^i(\omega_k) \end{bmatrix} = \boldsymbol{x}^{\mathrm{T}}\boldsymbol{H}^{\mathrm{T}}\boldsymbol{H}\boldsymbol{x} + 2\boldsymbol{g}^{\mathrm{T}}\boldsymbol{H}\boldsymbol{x} + \boldsymbol{g}^{\mathrm{T}}\boldsymbol{g} \tag{21}$$

is introduced using ω_k, where

$$\boldsymbol{H} := \begin{bmatrix} \alpha(\omega_1) \\ \vdots \\ \alpha(\omega_N) \end{bmatrix}, \ \boldsymbol{g} := \begin{bmatrix} \beta(\omega_1) \\ \vdots \\ \beta(\omega_N) \end{bmatrix}. \tag{22}$$

When $\boldsymbol{H}$ has full rank, $\boldsymbol{H}^{\mathrm{T}}\boldsymbol{H}$ is a non-singular matrix. Thus, $J < \gamma$ is represented by the LMI condition:

$$\begin{bmatrix} \gamma - 2\boldsymbol{g}^{\mathrm{T}}\boldsymbol{H}\boldsymbol{x} - \boldsymbol{g}^{\mathrm{T}}\boldsymbol{g} & \mathrm{x}^{\mathrm{T}}\boldsymbol{H}^{\mathrm{T}} \\ \boldsymbol{H}\boldsymbol{x} & \boldsymbol{I} \end{bmatrix} > 0 \tag{23}$$

by setting γ and using the Schur complement. The minimization problem of J is equivalent to a γ-minimization problem. The LMI condition of Eq. (23) is easy to solve as a convex problem.

3.4. Procedure of PFC design in the conventional method

The PFC design procedure is shown as follows. At Step 0, parameters and initial values used in iteration are specified. At Step 1, constants used after Step 1 are calculated by using parameters and initial values specified at Step 0. At Step 2, a matrix, $\boldsymbol{P}_a$, of the Lyapunov inequality is derived in order to guarantee the minimum phase property of the augmented system. At Step 3, a matrix, $\boldsymbol{P}_f$, of the Lyapunov inequality is derived in order to guarantee the stability of the PFC. At Step 4, coefficients of the PFC are derived by minimizing the objective function under the Lyapunov inequality to guarantee the minimum phase property of the augmented system, and the Lyapunov inequality to guarantee the stability of the PFC. At Step 5, Steps 2 through 4 are repeated until the objective function becomes small.

Step 0 The following initial parameters are specified:

(0a) The desired model, $G_r(s)$, is specified. $G_r(s)$ provides sufficiently high gain in the anti-resonance frequency band of the plant, $G_p(s)$, and has the ASPR property.

(0b) The degree of $G_f(s)$, n, is specified. Here, m is set to be $n-1$.

(0c) An initial PFC, $G_{f0}(s) = n_{f0}(s)/d_{f0}(s)$, is specified. $G_{f0}(s)$ must be a stable system and provide the ASPR property of $G_{a0}(s) = G_p(s) + G_{f0}(s)$ (Remark 1). $G_{f0}(s)$ is used as an initial PFC for the iteration.

(0d) The denominator polynomial, $d(s)$, of the weighting function $M(s)$ is specified.

(0e) The reference frequency data, ω_k, $k = 1, \cdots, N$, are specified.

Step 1 (1a) Using b_{n-1} of $n_{f0}(s)$, $b_{a_{m_a}}$ of Eq. (17) is derived and is used as a constant for the following iteration.

(1b) Using ω_k, $\boldsymbol{H}$ and $\boldsymbol{g}$ of Eq. (22) are derived.

Step 2 Using $n_{f0}(s)$ and $d_{f0}(s)$, $n_a(s)$ of Eq. (13) is derived and the matrix $\boldsymbol{A}_a$ of Eq. (15) is derived. Then, by solving the ϵ_a-minimization problem

$$\min_{\epsilon_a,\ \boldsymbol{P}_a} \ \epsilon_a \ \text{ s.t. } \ \boldsymbol{P}_a\boldsymbol{A}_a + \boldsymbol{A}_a^{\mathrm{T}}\boldsymbol{P}_a < 0, \quad \boldsymbol{P}_a > 0, \quad \boldsymbol{P}_a - \epsilon_a\boldsymbol{I} < 0, \tag{24}$$

$\boldsymbol{P}_a \in R^{m_a \times m_a}$ is obtained.

Step 3 The stability of $G_f(s)$ is guaranteed by a similar procedure for the minimum phase condition. Using $d_{f0}(s)$, the matrix $\boldsymbol{A}_f$,

$$\boldsymbol{A}_f = \begin{bmatrix} 0 & 1 & 0 & \cdots & 0 \\ 0 & 0 & 1 & \cdots & 0 \\ \vdots & \vdots & \ddots & \ddots & \vdots \\ 0 & 0 & \cdots & \cdots & 1 \\ -a_0 & -a_1 & \cdots & \cdots & -a_{n-1} \end{bmatrix}, \tag{25}$$

is derived. By solving the ϵ_f-minimization problem

$$\min_{\epsilon_f,\ \boldsymbol{P}_f} \ \epsilon_f \ \text{ s.t. } \ \boldsymbol{P}_f\boldsymbol{A}_f + \boldsymbol{A}_f^{\mathrm{T}}\boldsymbol{P}_f < 0, \quad \boldsymbol{P}_f > 0, \quad \boldsymbol{P}_f - \epsilon_f\boldsymbol{I} < 0, \tag{26}$$

$\boldsymbol{P}_f \in R^{n \times n}$ is obtained.

Step 4 Using $\boldsymbol{P}_a$ and $\boldsymbol{P}_f$ obtained in Steps 2 and 3, the γ-minimization problem

$$\min_{\gamma,\,\boldsymbol{x},\,\boldsymbol{A}_a,\,\boldsymbol{A}_f} \gamma \ \text{s.t.} \begin{bmatrix} \gamma - 2\boldsymbol{g}^{\mathrm{T}}\boldsymbol{H}\boldsymbol{x} - \boldsymbol{g}^{\mathrm{T}}\boldsymbol{g} & \boldsymbol{x}^{\mathrm{T}}\boldsymbol{H}^{\mathrm{T}} \\ \boldsymbol{H}\boldsymbol{x} & \boldsymbol{I} \end{bmatrix} > 0 \tag{27}$$

$$\boldsymbol{P}_a\boldsymbol{A}_a + \boldsymbol{A}_a^{\mathrm{T}}\boldsymbol{P}_a < 0 \tag{28}$$

$$\boldsymbol{P}_f\boldsymbol{A}_f + \boldsymbol{A}_f^{\mathrm{T}}\boldsymbol{P}_f < 0 \tag{29}$$

is solved for $\boldsymbol{A}_a$ and $\boldsymbol{A}_f$, where $\boldsymbol{A}_a$ and $\boldsymbol{A}_f$ are variables consisting of $\boldsymbol{x}$ and their structures are Eq. (15) and Eq. (25), respectively. Here, $G_f(s)$, which consists of the obtained solution, $\boldsymbol{x}$, is a stable system and gives the ASPR property of $G_a(s)$.
Step 5 Steps 2 through 4 are repeated until γ becomes sufficiently small. Here, $G_f(s) = n_f(s)/d_f(s)$ used in Steps 2 and 3 is an updated solution obtained in Step 4.
Remark 1: Increasing the gain of the PFC simplifies the design of the PFC which provides the ASPR property of $G_a(s)$.
Remark 2: At Step 4, $\boldsymbol{A}_a$ and $\boldsymbol{A}_f$ which minimize γ for $\boldsymbol{P}_a$ and $\boldsymbol{P}_f$ are obtained. When the procedure is executed iteratively by Step 5, and Eq. (24) and Eq. (26) using these $\boldsymbol{A}_a$ and $\boldsymbol{A}_f$ are solved in Steps 2 and 3, γ of Eq. (27) is invariant. Thus, γ does not deteriorate in Steps 2 and 3. Therefore, γ is guaranteed to decrease monotonically by this procedure.
At (1a) of Step 1, the leading coefficient, b_{n-1}, of the PFC is specified and is treated as a constant at the optimal problem. However, if b_{n-1} cannot be specified appropriately, the result of the frequency response fitting deteriorates. In order to treat b_{n-1} as a design parameter of the optimal problem, a method using a descriptor system is proposed in the following chapter.

4. Proposed method

4.1. Stability theorem of the descriptor system

A descriptor system is introduced in order to relax the requirement that $b_{a_{m_a}}$ is specified in advance. A transfer function for which the denominator is $n_a(s)$ is represented as the descriptor system (Shiotsuki, 2011)

$$\boldsymbol{E}_D\dot{\boldsymbol{x}}_D(t) = \boldsymbol{A}_D\boldsymbol{x}_D(t) + \boldsymbol{b}_D u_D(t), \tag{30}$$

$$\boldsymbol{E}_D = \begin{bmatrix} \boldsymbol{I}_{m_a} & \boldsymbol{0}_{m_a\times 1} \\ \boldsymbol{0}_{1\times m_a} & 0 \end{bmatrix},\ \boldsymbol{A}_D = \begin{bmatrix} 0 & 1 & 0 & \cdots & 0 \\ 0 & 0 & 1 & \cdots & 0 \\ \vdots & \vdots & \ddots & \ddots & \vdots \\ 0 & 0 & \cdots & \cdots & 1 \\ b_{a_0} & b_{a_1} & \cdots & \cdots & b_{a_{m_a}} \end{bmatrix},\ \boldsymbol{b}_D = \begin{bmatrix} 0 \\ 0 \\ \vdots \\ 0 \\ -1 \end{bmatrix} \tag{31}$$

where $\boldsymbol{A}_D$ is affine for all parameters in Eq. (31). The stability of the descriptor system is defined in the following.
Definition (Uezato and Ikeda, 1998; Katayama, 1999) It is assumed that $b_{a_{m_a}} \neq 0$. If the real part of all exponential modes is negative, the system of Eq. (30) is stable. Here, exponential modes are roots of $\det(s\boldsymbol{E}_D - \boldsymbol{A}_D) = 0$.
When $b_{a_{m_a}} \neq 0$, Eq. (30) is equivalent to the state equation of Eq. (14), and the exponential modes are equal to the modes of the state equation (Shiotsuki, 2011). Therefore, the stability of the descriptor system is equivalent to the stability of $n_a(s)$.
Theorem (Uezato and Ikeda, 1998) The system of Eq. (30) is stable if and only if there exist a $\boldsymbol{P}_D > 0 \in R^{(m_a+1)\times(m_a+1)}$ and $s_D \neq 0$ which satisfy

$$\boldsymbol{A}_D(\boldsymbol{P}_D\boldsymbol{E}_D^{\mathrm{T}} + \boldsymbol{v}_D s_D \boldsymbol{u}_D^{\mathrm{T}}) + (\boldsymbol{E}_D\boldsymbol{P}_D + \boldsymbol{u}_D s_D \boldsymbol{v}_D^{\mathrm{T}})\boldsymbol{A}_D^{\mathrm{T}} < 0 \tag{32}$$

where $\boldsymbol{v}_D$ and $\boldsymbol{u}_D$ are $(m_a+1)\times 1$ vectors composed of bases of Null$\boldsymbol{E}_D$ and Null$\boldsymbol{E}_D^{\mathrm{T}}$, respectively.
Proof Refer to the Uezato and Ikeda (1998).

By using Eq. (32) as a new restriction instead of Eq. (16), the requirement that $b_{a_{m_a}}$ or b_{n-1} is specified in advance is relaxed, i.e., it is not required to specify b_{n-1} in advance.

4.2. Procedure of PFC design in the proposed method

Since $b_{a_{m_a}}$ or b_{n-1} becomes a design parameter of the optimal problem, the proposed method eliminates procedure (1a) of Step 1 and sets $\tilde{\boldsymbol{x}} = [a_0, \ldots, a_{n-1}, b_0, \ldots, b_{n-1}]$. Then, the objective function, Eq. (21), is modified as follows:

$$\begin{aligned} J(\tilde{\boldsymbol{x}}) &= \sum_{k=1}^{N} \begin{bmatrix} E^r(\omega_k) & E^i(\omega_k) \end{bmatrix} \begin{bmatrix} E^r(\omega_k) \\ E^i(\omega_k) \end{bmatrix}, \\ &= \tilde{\boldsymbol{x}}^{\mathrm{T}}\tilde{\boldsymbol{H}}^{\mathrm{T}}\tilde{\boldsymbol{H}}\tilde{\boldsymbol{x}} + 2\tilde{\boldsymbol{g}}^{\mathrm{T}}\tilde{\boldsymbol{H}}\tilde{\boldsymbol{x}} + \tilde{\boldsymbol{g}}^{\mathrm{T}}\tilde{\boldsymbol{g}}, \end{aligned} \tag{33}$$

where $\tilde{\boldsymbol{H}}$ and $\tilde{\boldsymbol{g}}$ are coefficient matrices corresponding to $\tilde{\boldsymbol{x}}$. Furthermore, the stability condition of the descriptor is newly used. The proposed PFC design replaces Steps 1, 2, and 4 in the conventional procedure in Section 3.4 with the following Steps 1′, 2′, and 4′, respectively.

Step 1′ (1b′) Using ω_k, $\tilde{\boldsymbol{H}}$ and $\tilde{\boldsymbol{g}}$ of Eq. (33) are derived.

Step 2′ Using $n_{f0}(s)$ and $d_{f0}(s)$, $n_a(s)$ of Eq. (13) is derived and the matrix $\boldsymbol{A}_D$ of Eq. (31) is derived. Then, the ϵ_D-minimization problem

$$\min_{\epsilon_d,\ \boldsymbol{P}_D,\ s_D} \epsilon_D \ \text{s.t.}\ \boldsymbol{A}_D(\boldsymbol{P}_D\boldsymbol{E}_D^{\mathrm{T}} + \boldsymbol{v}_D s_D \boldsymbol{u}_D^{\mathrm{T}}) + (\boldsymbol{E}_D\boldsymbol{P}_D + \boldsymbol{u}_D s_D \boldsymbol{v}_D^{\mathrm{T}})\boldsymbol{A}_D^{\mathrm{T}} < 0,\ \ \boldsymbol{P}_D > 0,\ \ \boldsymbol{P}_D - \epsilon_D \boldsymbol{I} < 0 \tag{34}$$

is solved instead of Eq. (24), and $\boldsymbol{P}_D \in R^{(m_a+1)\times(m_a+1)}$ and $s_D \in R$ are obtained.

Step 4′ Using $\boldsymbol{P}_D$, s_D and $\boldsymbol{P}_f$ obtained in Steps 2′ and 3, the γ-minimization problem

$$\min_{\gamma,\ \tilde{\boldsymbol{x}},\ \boldsymbol{A}_D,\ \boldsymbol{A}_f,\ b_{a_{ma}}} \gamma \ \text{s.t.} \begin{bmatrix} \gamma - 2\tilde{\boldsymbol{g}}^{\mathrm{T}}\tilde{\boldsymbol{H}}\tilde{\boldsymbol{x}} - \tilde{\boldsymbol{g}}^{\mathrm{T}}\tilde{\boldsymbol{g}} & \tilde{\boldsymbol{x}}^{\mathrm{T}}\tilde{\boldsymbol{H}}^{\mathrm{T}} \\ \tilde{\boldsymbol{H}}\tilde{\boldsymbol{x}} & \boldsymbol{I} \end{bmatrix} > 0 \tag{35}$$

$$\boldsymbol{A}_D(\boldsymbol{P}_D\boldsymbol{E}_D^{\mathrm{T}} + \boldsymbol{v}_D s_D \boldsymbol{u}_D^{\mathrm{T}}) + (\boldsymbol{E}_D\boldsymbol{P}_D + \boldsymbol{u}_D s_D \boldsymbol{v}_D^{\mathrm{T}})\boldsymbol{A}_D^{\mathrm{T}} < 0 \tag{36}$$

$$\boldsymbol{P}_f\boldsymbol{A}_f + \boldsymbol{A}_f^{\mathrm{T}}\boldsymbol{P}_f < 0 \tag{37}$$

$$b_{a_{ma}} > 0 \tag{38}$$

is solved, where $\boldsymbol{A}_D$, $\boldsymbol{A}_f$, and $b_{a_{ma}}$ are variables which consist of $\tilde{\boldsymbol{x}}$, and their structures are Eq. (31), Eq. (25), and Eq. (17), respectively. Eq. (38) is newly added in order to guarantee condition III).

5. Experiments verification

5.1. Experimental system

The experimental system is a mechanical vibration system shown in Figs. 4 and 5. The system consists of a paddle, a 0.3 kg mass attached at L mm, a motor, and a rotary encoder. The approximated model of the system is shown in Fig. 6. The equation of motion is described as follows:

$$J_1\ddot{\theta}_1 + K\theta_1 - K\theta_2 + (D_1 + D_2)\dot{\theta}_1 - D_2\dot{\theta}_2 = u, \tag{39}$$

$$J_2\ddot{\theta}_2 + K\theta_2 - K\theta_1 + D_2\dot{\theta}_2 - D_2\dot{\theta}_1 = 0 \tag{40}$$

where $\theta_1(t)$ and $\theta_2(t)$ are the rotation angles of the rotary shaft and the weight, respectively, J_1 is the moment of inertia of the rotary shaft, and J_2 is the moment of inertia of the weight and the paddle, K is the equivalent spring constant of the vibration mode, and D_1 and D_2 are the viscosity coefficients of the motor shaft and the paddle, respectively. The control input, $u(t)$, is applied by the motor attached to the lower part of the rotary shaft. The control output, $\theta_1(t)$, is measured by the rotary encoder. Plants are denoted as $P_1(s)$, $P_2(s)$, and $P_3(s)$ when the attached locations of the weight are L_1, L_2, and L_3, respectively. Hereinafter, $P_2(s)$ is regarded as the nominal plant. Moreover, $P_1(s)$ and $P_3(s)$ are used as perturbed systems to verify the robustness of the SAC designed using the proposed method. The parameters of the plant and variables are shown in Table 1, and the values of L are shown in Table 2. The frequency responses of $P_1(s)$, $P_2(s)$, and $P_3(s)$ are shown in Fig. 7.

5.2. PD controller

The plants are not stable because each plant includes an integrator. Therefore, the minor PD controller, as shown in Fig. 8, is applied to the plants, which are stabilized by the PD control, where k_p is the proportional gain and k_d is the derivative gain, which are specified as $k_p = 3.5$ and $k_d = 1$, respectively. Figure 9 shows the frequency response of $G_{pi}(s)$ $(i = 1, 2, 3)$, where $G_{pi}(s)$ is the plant with the minor PD control for $P_i(s)$. The closed-loop system for $P(s) = P_2(s)$, $G_{p2}(s)$, is obtained as follows:

$$G_{p2}(s) = \frac{81.02(s^2 + 0.0009255s + 137.9)}{(s^2 + 17.38s + 416.6)(s^2 + 6.926s + 26.81)}. \tag{41}$$

$G_{p2}(s)$ is not ASPR because the relative degree is 2. In addition, $G_{p2}(s)$ includes the anti-resonance mode. The PFC is designed for the nominal plant $G_{p2}(s)$. $G_{p1}(s)$ and $G_{p3}(s)$ are obtained as follows:

$$G_{p1}(s) = \frac{81.02(s^2 + 0.01193s + 57.12)}{(s^2 + 20.41s + 262.3)(s^2 + 3.928s + 17.64)}, \tag{42}$$

$$G_{p3}(s) = \frac{81.02(s^2 + 0.001441s + 245.4)}{(s^2 + 14.24s + 540.5)(s^2 + 10.07s + 36.79)}. \tag{43}$$

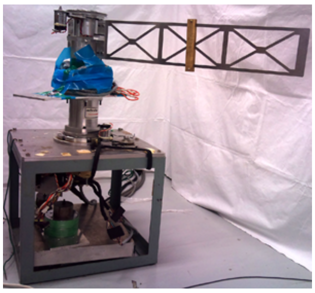

Fig. 4 Experimental system

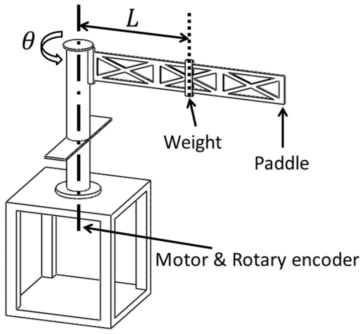

Fig. 5 Model of the plant is expressed. The motor rotates the paddle equipped the mass attached at L mm.

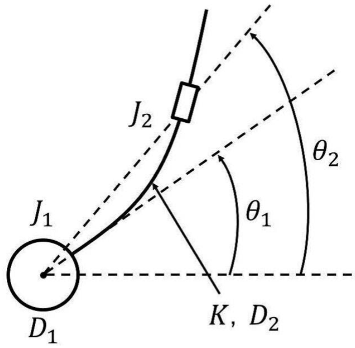

Fig. 6 Approximated model of the plant is expressed. J_1 and J_2 are the moment of inertia of the rotary shaft and the weight, respectively, K is the spring constant, and equivalent D_1 and D_2 are the viscosity coefficients of the motor shaft and the paddle, respectively.

Table 1 Parameters of the plant

Moment of inertia of the rotary shaft	J_1	0.0422 [kg·m^2]
Moment of inertia of the weight and the paddle	J_2	0.1081 [kg·m^2]
Equivalent spring constant of the vibration mode	K	14.9[Nm/rad]
Viscosity coefficient of the motor shaft	D_1	0.05 [Nms/rad]
Viscosity coefficient of the paddle	D_2	0.0001 [Nms/rad]
Control input (Torque)	u	-[Nm]
Rotation angle of the rotary shaft	θ_1	-[rad]
Rotation angle of the weight	θ_2	-[rad]

Table 2 Perturbed value of L

Plant	L [mm]
P_1	435
P_2	290
P_3	145

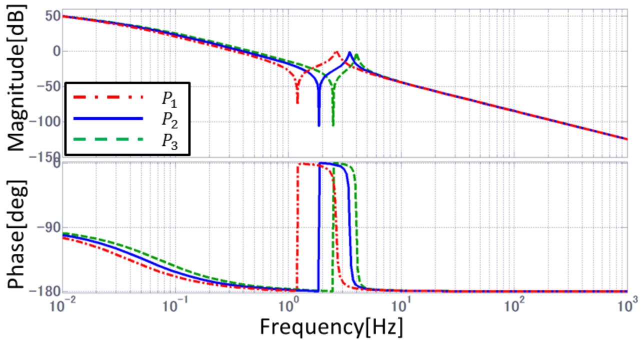

Fig. 7 Bode plots of $P_1(s)$, $P_2(s)$, and $P_3(s)$ are expressed. The chained, solid, and broken lines are $P_1(s)$, $P_2(s)$, and $P_3(s)$, respectively.

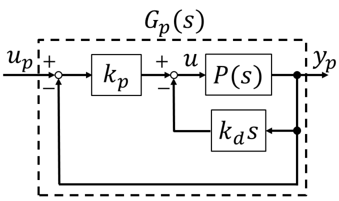

Fig. 8 Modified plant with minor feedback is expressed. k_p is the proportional gain and k_d is the derivative gain.

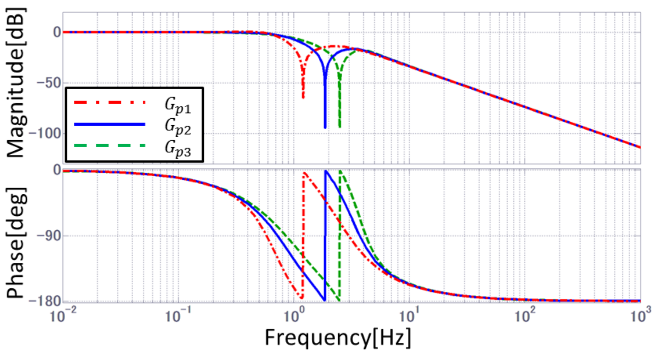

Fig. 9 Bode plots of $G_{p1}(s)$, $G_{p2}(s)$, and $G_{p3}(s)$ are expressed. The chained, solid, and broken lines are $G_{p1}(s)$, $G_{p2}(s)$, and $G_{p3}(s)$, respectively.

5.3. PFC design

5.3.1. Design using the proposed method

(Step 0): (0a) The desired model is specified as follows:

$$G_r(s) = \frac{6.371s^2 + 416.3s + 1006}{s^3 + 24.12s^2 + 211.9s + 838.4}. \tag{44}$$

Figure 10 shows the frequency response of $G_r(s)$. The dotted and solid lines indicate $G_{p2}(s)$ and $G_r(s)$, respectively. $G_r(s)$ has large gain at the anti-resonance frequency of $G_{p2}(s)$. (0b) We specify $n = 3$. (0c) The initial value of the PFC is specified as follows:

$$G_{f0}(s) = \frac{n_{f0}(s)}{d_{f0}(s)} = \frac{b_{n-1}(s^2 + 2 \cdot 20\pi s + (20\pi)^2)}{(s + 10)(s^2 + 2 \cdot 40\pi s + (40\pi)^2)}, \quad b_{n-1} = 20. \tag{45}$$

(0d) The denominator polynomial of $M(s)$ is specified as $d(s) = d_{f0}(s)$. (0e) Reference frequency data, ω_k, are specified as the following nine points: $\omega_k = 2\pi f_k,\ f_k \in \{f \mid 1\times10^{-4},\ 1\times10^{-3},\ 1\times10^{-2},\ 0.5,\ 1,\ 2,\ 1\times10^{2},\ 1\times10^{3},\ 1\times10^{4}\}$ [Hz]. (Step 1′): (1b′) Using ω_k, $\tilde{\boldsymbol{H}}$ and $\tilde{\boldsymbol{g}}$ of Eq. (33) for $\tilde{\boldsymbol{x}}$ are derived. Steps 2′ through 4′ are iterated 1,000 times. The PFC by the proposed method is obtained as follows:

$$G_f(s) = \frac{6.380s^2 + 359.1s + 247.1}{s^3 + 22.55s^2 + 165.9s + 770.1} \tag{46}$$

Figure 10 shows the frequency response of $G_a(s)$ using the PFC of Eq. (46). The broken line indicates $G_a(s)$. According to Fig. 10, the frequency response of $G_a(s)$ is well matched to that of $G_r(s)$. The convergence trajectory of γ is shown in Fig. 11. γ is reduced by the iteration.

5.3.2. Comparison with the conventional method In this section, the performances of the proposed and conventional method are compared. In the conventional method (Tanemura, et al., 2013), the leading coefficient of $G_a(s)$, $b_{a_{m_a}}$, must be given in advance in order to modify Eq. (15) to be affine. In other words, b_{n-1} must be specified in advance because $b_{a_{m_a}}$ is given by Eq. (17). b_{n-1} is determined such that $b_{a_{m_a}}$ is equal to $G_r(s)$. As such, condition III) of the ASPR condition is satisfied. In addition, the frequency response of $G_a(s)$ can fit that of $G_r(s)$ in the high-frequency band because the band depends on the leading coefficient. The PFC is designed for the following two cases.

$$\text{Case 1: } b_{n-1} = 6.371, \quad \text{Case2: } b_{n-1} = 10 \tag{47}$$

An initial value of the PFC is Eq. (45) with specified b_{n-1} in Eq. (47). Steps 2 through 4 are iterated 10 times. PFC is obtained as follows:

$$\text{Case 1: } G_f(s) = \frac{6.371s^2 + 315.7s + 101.9}{s^3 + 18.51s^2 + 154.9s + 527.4}, \quad \text{Case2: } G_f(s) = \frac{10s^2 + 211.0s + 54.11}{s^3 + 12.79s^2 + 113.8s + 295.5} \tag{48}$$

Figure 12 shows the frequency responses of $G_a(s)$, which are constituted using the PFC of Eq. (48). The solid, broken, and dotted lines show $G_r(s)$, $G_a(s)$ for Case 1, and $G_a(s)$ for Case 2, respectively. Case 1 achieves sufficient fitting of the frequency response, but the fitting for Case 2 is insufficient. The convergence trajectories of γ are shown in Fig. 13. The broken and dotted lines indicate the results for Cases 1 and 2, respectively. The iteration of times and the fitting rates (Adachi, 2009) in the proposed method and Cases 1 and 2 are shown Table 3. The proposed method requires many more iterations than the conventional method. The performance of the proposed method is approximately equal to that of Case 1 with respect to the fitting rate. In contrast, the fitting rate decreases when the leading coefficient is specified inappropriately, as in Case 2. Accordingly, although the proposed method requires numerous iterations, good matching results are obtained regardless of the initial value setting of the leading coefficient, b_{n-1}. In addition, if the PFC is designed such as $G_f(s) = G_r(s) - G_p(s)$ by the method proposed by Mizumoto, et al. (2010), order of the PFC is 7-th, however, the order of the PFC designed by the proposed method is 3-rd. The proposed method can design the specified low order PFC compared with the method proposed by Mizumoto, et al. (2010).

5.4. Simulation results

The vibration suppression effect of the SAC designed using the proposed method is verified through numerical simulations. The reference input, $u_m(t)$, is assumed to be a square wave for which the amplitude and period are 1 and 50 s, respectively. The following are used as parameters of SAC controllers:

$$G_m(s) = \frac{\omega_n^2}{s^2 + 2 \cdot 0.707\omega_n s + \omega_n^2}, \quad \omega_n = 0.8 \cdot 2\pi \tag{49}$$

$$\boldsymbol{\Gamma}_P = \mathrm{diag}\left\{10,\quad 1,\quad 1,\quad 0.1\right\}, \quad \boldsymbol{\Gamma}_I = \mathrm{diag}\left\{100,\quad 1,\quad 1,\quad 1\right\} \tag{50}$$

$$\sigma(t) = \frac{e_a^2(t)}{1 + e_a^2(t)}\sigma_1 + \sigma_2, \quad \sigma_1 = 1\times10^{-2}, \sigma_2 = 1\times10^{-5} \tag{51}$$

$$\boldsymbol{k}_I(0) = \left[-20,\quad 0,\quad 0,\quad 1\right]^{\mathrm{T}} \tag{52}$$

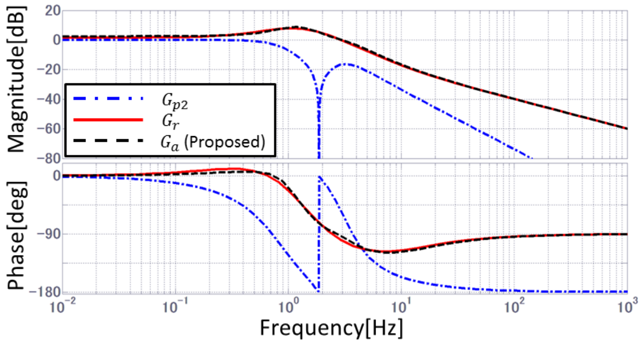

Fig. 10 Bode plot of $G_{p2}(s)$, $G_r(s)$ and $G_a(s)$ for proposed method are expressed. The chained, solid, and broken lines are $G_{p2}(s)$, $G_r(s)$, and $G_a(s)$, respectively. The frequency response of $G_a(s)$ is well matched to that of $G_r(s)$.

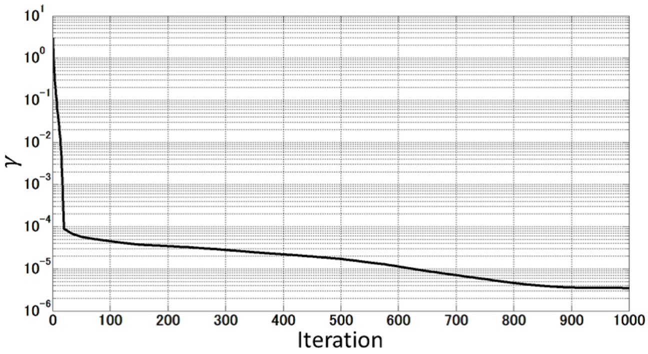

Fig. 11 Trajectory of γ is expressed. γ is reduced by the iteration.

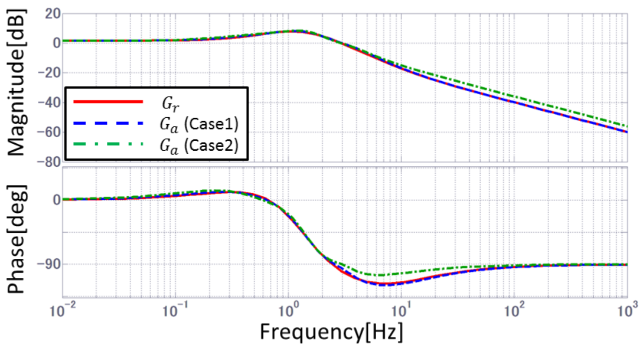

Fig. 12 Bode plots of $G_r(s)$, $G_a(s)$ for Case 1, and $G_a(s)$ for Case 2 are expressed. The solid, broken, and chained lines are $G_r(s)$, $G_a(s)$ for Case 1, and $G_a(s)$ for Case 2, respectively. Case 1 achieves sufficient fitting of the frequency response, but the fitting for Case 2 is insufficient.

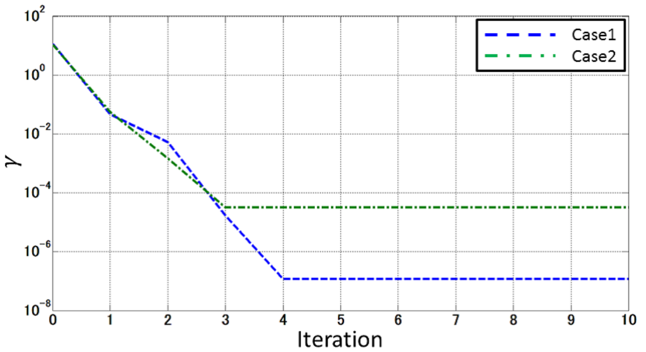

Fig. 13 Trajectories of γ for Cases 1 and 2 are expressed. γ are reduced by the iteration.

Table 3 Performance of the Proposed Method and Cases 1 and 2

	Proposed method	Case1	Case2
Iteration of times	1000	10	10
Fitting rate[%]	96.0	98.6	86.8

An approximate differentiator is used for the PD controller. Figures 14 and 15 show the control input, $u(t)$, and the control output, $y_p(t)$, at $P_2(s)$. The proposed method suppresses the vibration of the input because $G_a(s)$ does not include the anti-resonance. As a result, the vibration does not affect the output in the proposed method.

5.5. Experimental results

5.5.1. Verification of vibration suppression The vibration suppression effect of the SAC designed using the proposed method is verified experimentally. Here, $G_m(s)$ and $G_f(s)$ are discretized by the zero-order hold with a sampling period of 2 ms. The derivative of the PD controller is discretized by the bilinear transformation. Also, $k_I(t)$ of Eq. (6) and Eq. (8) is integrated using the forward Euler method. The control input, $u(t)$, and the control output, $y_p(t)$, for $P_2(s)$ are shown in Figs. 16 and 17. The proposed method suppresses the vibration of the input similarly to the simulation result. Consequently, the vibratory output does not occur when using the proposed method.

5.5.2. Verification of the robustness Figures 18 through 21 show $u(t)$ and $y_p(t)$ for $P_1(s)$ and $P_3(s)$. Figures 18 and 19 show the time responses of $P_1(s)$, and Figs. 20 and 21 show the time responses of $P_3(s)$. In both cases, the proposed method suppresses the vibration of the input. As a result, the vibratory output does not appear. The proposed method is robust because the proposed method can suppress the vibration even if the plant is subjected to perturbation. The experimental results reveal the effectiveness of the proposed method with the PFC design to suppress vibration.

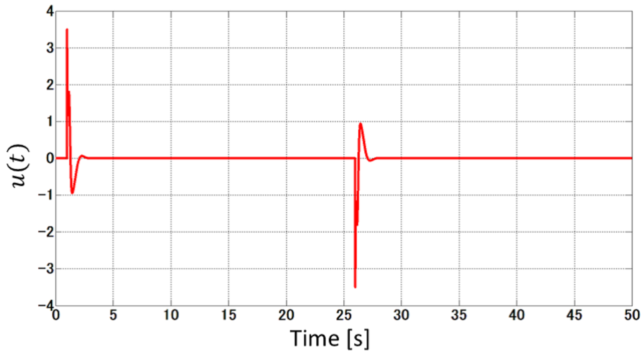

Fig. 14 Time history of $u(t)$ at $P_2(s)$ in simulation is expressed. The proposed method suppresses the vibration of $u(t)$ because $G_a(s)$ does not include the anti-resonance.

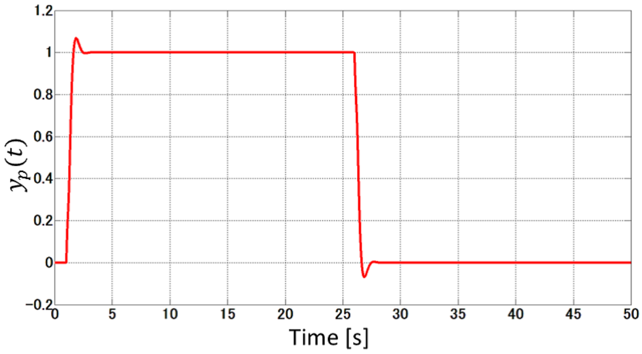

Fig. 15 Time response of $y_p(t)$ at $P_2(s)$ in simulation is expressed. The proposed method suppresses the vibration of $y_p(t)$.

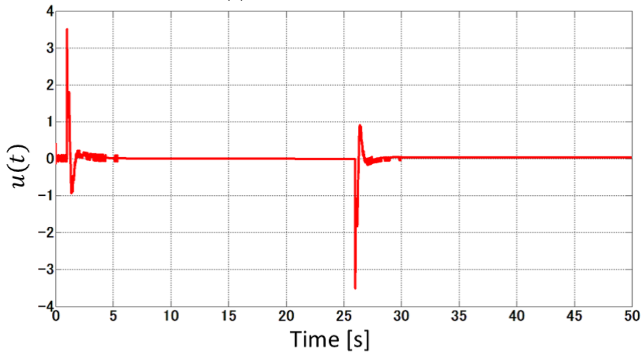

Fig. 16 Time history of $u(t)$ at $P_2(s)$ in experiment is expressed. The proposed method suppresses the vibration of $u(t)$.

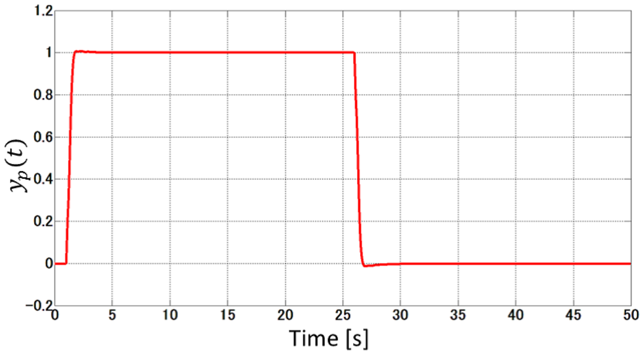

Fig. 17 Time response of $y_p(t)$ at $P_2(s)$ in experiment is expressed. The proposed method suppresses the vibration of $y_p(t)$.

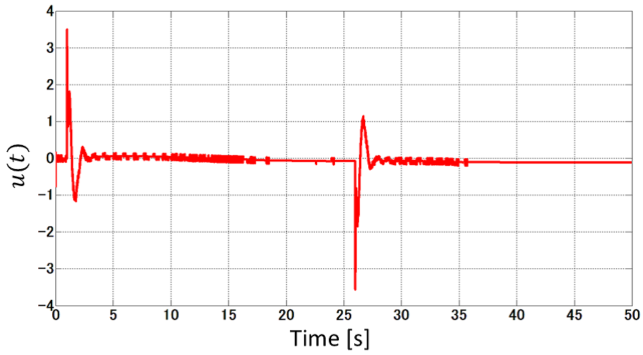

Fig. 18 Time history of $u(t)$ at $P_1(s)$ in experiment is expressed. The proposed method suppresses the vibration of $u(t)$.

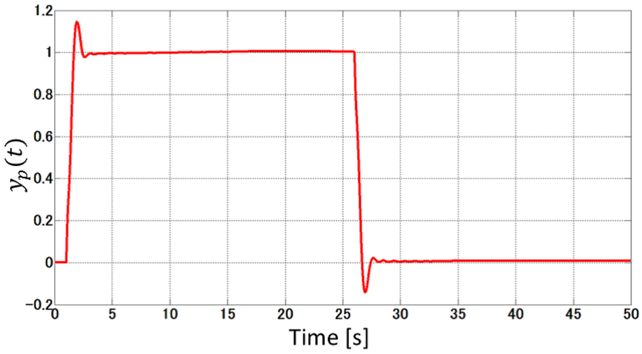

Fig. 19 Time response of $y_p(t)$ at $P_1(s)$ in experiment is expressed. The proposed method suppresses the vibration of $y_p(t)$.

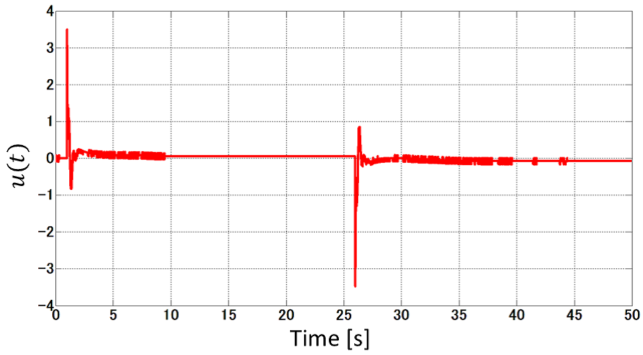

Fig. 20 Time history of $u(t)$ at $P_3(s)$ in experiment is expressed. The proposed method suppresses the vibration of $u(t)$.

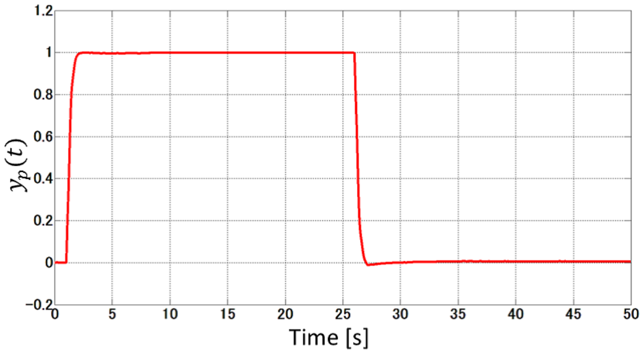

Fig. 21 Time response of $y_p(t)$ at $P_3(s)$ in experiment is expressed. The proposed method suppresses the vibration of $y_p(t)$.

6. Conclusion

The present paper proposes a PFC design method based on frequency response fitting for continuous-time SISO systems. The conditions of frequency response fitting, the ASPR property, and the stability are derived as BMI/LMI conditions, and the BMI/LMI problem is solved using an iterative procedure. The present paper introduces the description of a descriptor system instead of the state space representation. Then, the stability theorem of a descriptor system is used in order to guarantee the ASPR property. The proposed method can treat all coefficient of the PFC as design parameters of the optimal problem because of redundancy of a descriptor system. An SAC for a mechanical vibration system is designed using the proposed method. The proposed method provides good frequency response fitting for PFC design. The experimental results reveal that the SAC designed using the proposed method suppresses the vibratory input and output, even if the plant is subjected to perturbation.

References

Adachi, S., Fundamentals of system identification, Tokyo Denki University Press (2009).(in Japanese)

Chida, Y. and Nishimura, T., Discretization method of continuous-time controllers based on frequency response fitting, SICE Journal of Control, Measurement, and System Integration, Vol.1, No.4 (2008), pp.299-306.

Hino, M., Iwai, Z., Fukushima. K. and Wakamiya. R., An active vibration control by means of a simple adaptive control method, Transactions of the Japan Society of Mechanical Engineers Series C, Vol.58, No.548 (1992), pp.1034-1040.(in Japanese)

Katayama, T., Optimal Control of Linear Systems: An Introduction to Descriptor Systems, Kindaikagaku (1999).(in Japanese)

Kyoizumi, K., Fujita, Y. and Ebihara, Y., Simple adaptive control method with automatic tuning of PFC and Its application to positioning control of a pneumatic servo system, Transactions of the Institute of Systems, Control and Information Engineers, Vol.14, No.3 (2001), pp.102-109.(in Japanese)

Mizumoto, I., Ikeda, D., Hirahata, T. and Iwai, Z., Design of discrete time adaptive PID control systems with parallel feedforward compensator, Control Engineering Practice, Vol.18, No.2 (2010), pp.168-176.

Mizumoto, I. and Iwai, Z., Recent trends on simple adaptive control (SAC), Journal of the Society of Instrument and Control Engineers, Vol.40, No.10 (2001), pp.723-728.(in Japanese)

Ohtomo, A., Iwai, Z., Nagata, M., Uchida, H. and Komera, Y., SAC (simple adaptive control) with PID and adaptive disturbance compensation for actuator composed of artificial rubber muscles, Transactions of the Japan Society of Mechanical Engineers Series C, Vol.63, No.605 (1997), pp.166-173.(in Japanese)

Shiotsuki, T., Analysis of linear systems, Corona Publishing (2011).(in Japanese)

Tanemura, M., Chida, Y. and Ikeda, Y., PFC design method using linear matrix inequality, the 56th Japan Joint Automatic Control Conference(2013), pp.295-300.(in Japanese)

Tanemura, M., Yamashiro, T., Chida, Y. and Maruyama, N., An issue of SAC for application to a plant including anti-resonance and improvement by PFC design, Transactions of the Japan Society of Mechanical Engineers, Vol.81, No.824 (2015), pp.1-12.(in Japanese)

Uezato, E. and Ikeda M., A strict LMI condition for stability of linear descriptor systems and its application to robust stabilization, Transactions of the Society of Instrument and Control Engineers, Vol.34, No.12 (1998), pp.1854-1860.(in Japanese)

Yamashiro, T. and Chida, Y., Simple adaptive control systems design for mechanical vibration systems including antires-onance, The Society of Instrument and Control Engineers Control Division (CD-ROM), Vol.12 (2012), pp.13:40-15:40.(in Japanese)